from selective cleavage of the least hindered bond of the cyclopropane. Elimination of water ($SOCl_2$, C_5H_5N, 0 °C, 92%) followed by epoxidation (MCPBA, CH_2Cl_2, room temperature, 87%) gave the crystalline epoxide **13**[9] (mp 189–189.5 °C dec) where the sulfone group at C(1) controls the stereochemistry of the epoxidation and subsequently of the hydroxyl group at C(9).

Deprotection of the epoxide **13** was accomplished by sequential acid (10% $HClO_4$, acetone, 35 °C) and base (DBU, CH_2Cl_2) treatment to give the unusual dienone **14**[9] in 91% yield. Hydrogenolysis of the allylic epoxide with sodium naphthalenide (DME, −45 °C) produces a mixture of olefin isomers after protonation which isomerize (catalytic DBU, CH_2Cl_2, room temperature, 52% overall yield) to a single crystalline dienone alcohol **15**[9,15] (mp 127–128 °C). The 11-Hz coupling constant between H(8) and H(9) supports the assigned stereochemistry.[3]

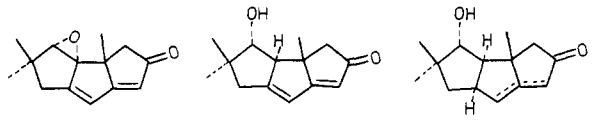

14 15 16 β,γ 17 α,β

The dienone **15** offers a splendid opportunity to introduce the remaining hydroxyl group since dissolving metal reduction and kinetic protonation will produce directly the β,γ-unsaturated enone **16** that is required. Indeed, lithium in liquid ammonia reduction followed by quenching into a pH 5.8 buffer gave an 80:20 ratio of **16** and **17**. Without manipulation, this mixture was chemoselectively epoxidized[16] (MCPBA, CH_2Cl_2) and the crude epoxide directly isomerized (DBU, CH_2Cl_2) to the allylic alcohol **18**,[9,15] mp 156–158 °C, in overall 63% yield and recovered α,β-enone **17** in overall 19% yield. The latter exhibited spectral properties identical with those of an authentic sample.[3c] Since **17** in principle can be deconjugated to reform **16** by a procedure similar to that employed in the other syntheses of coriolin,[3] this minor byproduct is also useful along the synthetic route. Crystalline diol **18**, available in 15 steps from enedione **5** in an overall yield of 5.3%, requires only α-methylenation and epoxidation to be converted into coriolin (**1**).

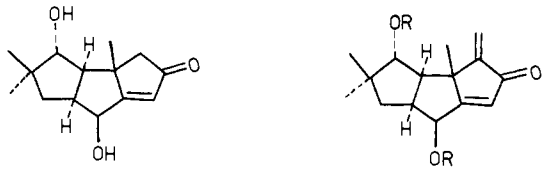

18 19 R=TMS 20 R=H

(15) **11**: ^1H NMR ($CDCl_3$, 270 MHz) δ 1.54 (3 H, s), 1.75 (1 H, br d), 2.31 (1 H, br d), 2.53 (1 H, d), 2.63 (1 H, d), 2.8–3.2 (4 H, m), 2.93 (3 H, s), 3.06 (3 H, s), 3.34 (1 H, s, exchanges with D_2O), 3.39 (1 H, br d), 3.50 (1 H, br d), 3.90 (4 H, m), 4.94 (1 H, br s), 4.97 (1 H, br s); ^{13}C NMR ($CDCl_3$, 19 MHz) δ 146.5, 113.9, 107.8, 94.6, 78.3, 76.6, 64.1 (two carbons), 59.9, 48.9, 46.2, 45.4, 44.2, 40.4, 39.7, 39.0, 19.0; IR ($CHCl_3$) 3500 br, 1670 cm^{-1}, no carbonyl; MS, *m/e* calcd for $C_{17}H_{26}O_7S_2$ 406.1113; found 406.1120. Anal. Calcd for C, H. **12**: ^1H NMR ($CDCl_3$, 270 MHz) δ 1.19 (3 H, s), 1.33 (3 H, s), 1.52 (3 H, s), 1.5–3.0 (10 H, m), 3.00 (3 H, s), 3.08 (3 H, s), 3.64 (1 H, s, exchanges w/D_2O), 3.92 (4 H, m); ^{13}C NMR ($CDCl_3$, 50.1 MHz) 114.8, 98.5, 78.4; 76.7, 64.4, 64.2, 58.5, 52.7, 51.6, 47.7, 45.9, 43.5, 40.3, 39.5, 37.4, 32.0, 31.8, 20.4; IR ($CHCl_3$) 3500 cm^{-1} br. **15**: ^1H NMR ($CDCl_3$, 270 MHz) 1.07 (3 H, s), 1.17 (3 H, s), 1.24 (3 H, s), 2.13 (1 H, br s), 2.1–2.6 (4 H, m), 3.03 (1 H, br d, *J* = 11 Hz), 3.80 (1 H, d, *J* = 11 Hz), 5.61 (1 H, s), 6.15 (1 H, br d, *J* = 2 Hz); ^{13}C NMR ($CDCl_3$, 50.1 MHz), 210.0 (s), 197.1 (s), 167.9 (s), 117.2 (d), 115.4 (d) 76.9 (d), 64.1 (d), 55.1 (s), 49.8 (t), 44.7 (s), 40.0 (t), 27.8, (q) 24.9 (q), 22.5 (q); IR ($CHCl_3$) 3600, 3500 br, 1685, 1600 cm;$^{-1}$ MS, *m/e* calcd for $C_{14}H_{18}O_2$, 218.1302; found 218.1306. Anal. Calcd for $C_{14}H_{18}O_2$: C, H. **18**: ^1H NMR ($CDCl_3$, 270 MHz) δ 0.95 (3 H, s), 1.10 (3 H, s), 1.45 (3 H, s), 1.48 (1 H, dd, *J* = 13, 9 Hz), 1.85 (1 H, dd, *J* = 13, 10 Hz), 2.22 (1 H, dd, *J* = 12, 9 Hz), 2.38 (1 H, d, *J* = 17 Hz), 2.52 (1 H, d, *J* = 17 Hz), 2.73 (1 H, m), 3.81 (1 H, d, *J* = 9 Hz), 4.65 (1 H, d, *J* = 6 Hz), 5.84 (1 H, s); ^{13}C NMR ($CDCl_3$, 50 MHz) δ 210.8 (s), 190.9 (s), 123.8 (d), 81.2 (d), 68.7 (d), 56.6 (d), 56.1 (t), 47.8 (s), 45.0 (d), 44.3 (s), 35.2 (t), 26.6 (q), 24.9 (q), 20.4 (q); IR ($CHCl_3$) 3600, 3500 br, 1708, 640 cm^{-1}; MS, *m/e* calcd for $C_{14}H_{20}O_3$, 236.1407; found 236.1412. Anal. Calcd for $C_{14}H_{20}O_3$: C, H.

(16) Enone **17** was not epoxidized under these conditions. See ref 3b,c.

Formation of the kinetic enol silyl ether (LDA, THF–HMPA, then Me_3SiCl) of the bis(trimethylsilyl) ether of **18** (*O,N*-bis-(trimethylsilyl)trifluoroacetamide, DMF, 40 °C) followed directly by reaction with dimethylmethyleneammonium iodide (Eschenmoser's salt)[17] in refluxing chloroform gave the corresponding Mannich base. Quaternization of the crude product (CH_3I, ether, room temperature) and elimination (DBU, CH_2Cl_2, room temperature) delivered the bis(trimethylsilyl) ether of the methylenated product **19** (46% overall yield from **18**). While standard desilylation methods tended to destroy the molecule, pyridine–polyhydrogen fluoride[18] in THF smoothly accomplished the final unmasking to give dienone **20** (>85% yield), the penultimate intermediate in all of the previous syntheses of coriolin and identical in all respects to an authentic sample.[19] The completion of the synthesis of **20** then constitutes a completion of the synthesis of coriolin since Danishefsky and his group successfully epoxidized **20** either in a one-step nonstereoselective or four-step stereoselective procedure to produce **1**.

The synthesis of coriolin clearly demonstrates the utility of the enedione **5** and methylenecyclopentane annulation in the total synthesis of polycondensed cyclopentanoid natural products. Its success provides impetus to convert the key tricycle **11** to other members of the family.

Acknowledgment. We thank the National Science Foundation and the National Cancer Institute of the National Institutes of Health for their generous financial support of our programs and the latter for a postdoctoral fellowship award to D.P.C. We thank Dr. S. Ikegami for spectral data for **18** and especially express our gratitude to Professor S. Danishefsky for not only providing comparison spectra but also a sample of **20** and a preprint of his full paper.

(17) Danishefsky, S.; Prisbylla, M.; Lipisko, B. *Tetrahedron Lett.* **1980**, 805. Holy, N.; Fowler, R.; Burnett, E.; Lorenz, R. *Tetrahedron* **1979**, *35*, 613. Danishefsky, S.; Kitahara, K.; McKee, R.; Schuda, P. F. *J. Am. Chem. Soc.* **1976**, *98*, 6717. Roberts, J. L.; Borromeo, P. S.; Poulter, C. D. *Tetrahedron Lett.* **1977**, 1621.

(18) Caldwell, C. G. Ph.D. thesis, University of Wisconsin, 1981. Independent of our work Nicolaou reported the use of this desilylation method. See: Nicolaou, K. C.; Seitz, S. P.; Pavia, M. R. *J. Am. Chem. Soc.* **1981**, *103*, 1222. Nicolaou, K. C.; Seitz, S. P.; Pavia, M. R.; Petasis, N. A. *J. Org. Chem.* **1979**, *44*, 4011.

(19) Compound **20** was identical (analytical TLC, IR, 270-MHz NMR, MS) to a sample kindly provided by Professor S. Danishefsky.

Hopping and Delocalized Electrons in Class II Mixed-Valence Oxovanadates

Subhash P. Harmalker and Michael T. Pope*

Department of Chemistry, Georgetown University
Washington, D.C. 20057

Received June 19, 1981

Mixed-valence compounds that can be described in terms of partially trapped discrete valence states (class II in the Robin–Day scheme[1]) attract considerable current interest in view of the insight they can provide for electron transfer and exchange processes.[2] Theoretical models[1,3] for mixed-valence compounds distinguish between "delocalized" and "trapped" descriptions, the former implying a ground-state or resonance averaging of valences and the latter implying the possibility of thermally activated intramolecular electron hopping. Although it has been presumed that all trapped valence state compounds are delocalized to some extent in order to account for the observation of intervalence charge transfer (IT) transitions in their optical spectra, the complexes reported here are the first examples of mixed-valence compounds

(1) Robin, M. B.; Day, P. *Adv. Inorg. Chem. Radiochem.* **1967**, *10*, 247.
(2) Meyer, T. J. "Mixed Valence Compounds"; Brown, D. B., ed.; D. Reidel Publishing Co.: Dordrecht, The Netherlands, 1980; p 75.
(3) (a) Hush, N. S. *Prog. Inorg. Chem.* **1967**, *8*, 357. (b) Piepho, S. B.; Krausz, E. R.; Schatz, P. N. *J. Am. Chem. Soc.* **1978**, *100*, 2996. Wong, K. Y.; Schatz, P. N.; Piepho, S. B. *Ibid.* **1979**, *101*, 2793.

0002-7863/81/1503-7381$01.25/0

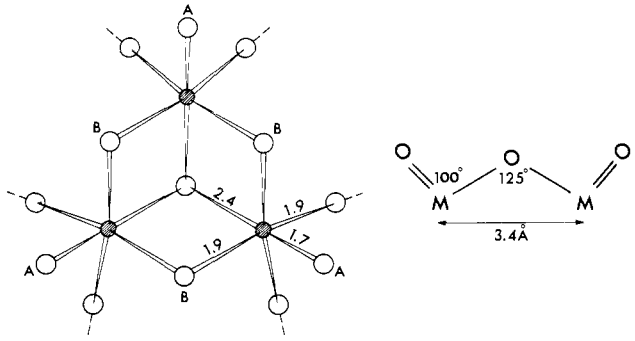

Figure 1. One of the two W_3O_{13} "caps" in the structure of α-$P_2W_{18}O_{62}^{6-}$ viewed along the anion's C_3 axis. Metal atoms are indicated by dark circles, terminal oxo oxygens by O_A, and intracap-bridging oxygens by O_B. Approximate dimensions are taken from ref 5 and pertain to a W_3O_{13} group. Complexes V_2 and V_3 contain analogous WV_2O_{13} and V_3O_{13} groups, in which bond lengths and angles are expected to differ little from those shown.

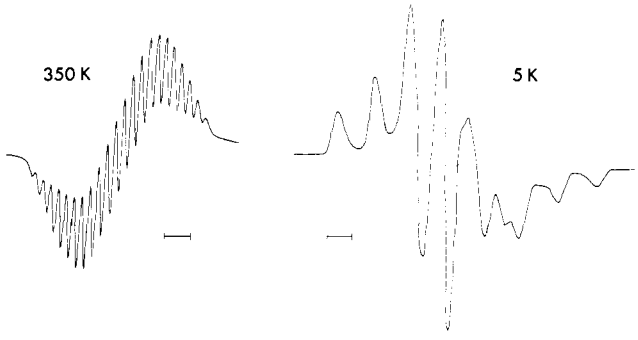

Figure 2. X-band ESR spectra of V_3 complex at pH 11, recorded in aqueous buffer at 350 K and in aqueous glycerol glass at 5 K. Scale bars represent 100 G.

which unequivocally show both electron hopping *and* significant resonance delocalization. The compounds also show a diminution in the apparent electron exchange activation energy from a high-temperature (>350 K) to a low-temperature (<200 K) regime.[4]

The compounds in question are heteropoly tungstate anions that contain two and three vanadium atoms. $P_2W_{16}V^{IV}V^{V}O_{62}^{9-}$ ("V_2"), $P_2W_{15}V^{IV}V^{V}_2O_{62}^{10-}$ ("V_3"), and $P_2W_{15}V^{IV}V^{V}_2O_{62}H^{9-}$ ("HV_3"). These polyanions have the overall "Dawson" structure[5] observed for α-$P_2W_{18}O_{62}^{6-}$, with vanadium atoms replacing tungstens in one of the two W_3O_{13} end "caps" illustrated in Figure 1.[6] The mixed-valence chemistry in these anions is effectively restricted to the vanadium atoms, although the optical spectra of the three complexes also show heteronuclear ($V^{IV} \rightarrow W^{VI}$) IT bands at energies above ca. 17 000 cm^{-1}.

The X-band electron spin resonance (ESR) spectra of V_3 at 350 and 5 K are shown in Figure 2. The 22-line high-temperature spectrum (a = 33 G) is consistent with rapid (>ca. 10^8 s^{-1}) intramolecular electron hopping among three equivalent $^{51}V(I = {}^7/_2)$ nuclei, and the low-temperature spectrum shows that the electron is trapped on a single vanadium nucleus.[7] The line width of the spectrum at 5 K is exceptionally broad[8] and the spectrum

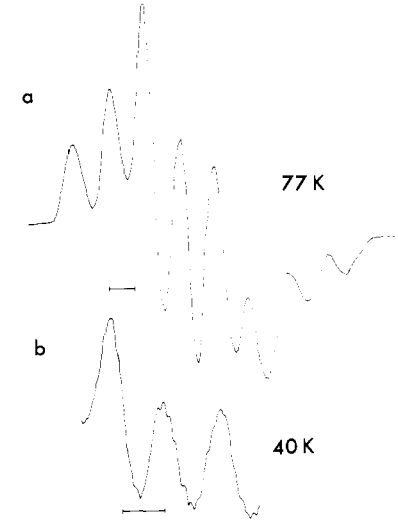

Figure 3. X-band ESR spectra of HV_3 recorded in 50% aqueous glycerol glass, pH 4.75: (a) Full spectrum at 77 K; (b) expanded central portion of spectrum at 40 K showing superhyperfine structure. Scale bars represent 100 G.

is unchanged between 5 and ca. 85 K. We thus attribute the broad lines to unresolved superhyperfine structure derived from partial electron delocalization on the two equivalent neighboring vanadium nuclei. Above 85 K the lines broaden still further and eventually coalesce. In the range 107–197 K the line width variation can be fitted to an Arrhenius plot and yields an activation energy for electron hopping (E_{th}) of 0.60 ± 0.14 kJ mol^{-1}. This value should be contrasted with that (39.6 kJ mol^{-1}) estimated from the energy of the optical IT band (E_{op} = 13 200 cm^{-1}) employing the relationship $E_{th} \simeq {}^1/_4 E_{op}$.[3a] The latter equation is valid only when delocalization is minimal and when $kT \gg \hbar\omega$ for the molecular vibrations which are coupled to the electron transfer.[1,3] Although delocalization is not insignificant and although V–O stretching vibrations in polyanions fall in the range 700–1000 cm^{-1}, we regard the 39.6 kJ mol^{-1} value as a high-temperature limit since the position of the IT band is unchanged between 77 and 300 K.

Protonation of V_3 to HV_3 occurs below pH 9 and may be detected by pronounced and reversible changes in ESR and optical spectra. For reasons to become clear later it is proposed that protonation occurs at one of the three O_B sites (Figure 1). The frozen-glass ESR spectra of HV_3 and of V_2 at 77 K are indistinguishable. These spectra are similar in appearance to, but have g and a values different from, that of V_3 and therefore indicate an electron trap site of slightly different symmetry.[9] When the temperature is lowered to 40 K, the spectra of both HV_3 and V_2 show clear evidence of superhyperfine structure, $a_{SHF} \approx 10$ G; see figure 3. Since the splitting is the same in both compounds, it appears that only one other vanadium nucleus is involved in HV_3. This can be accounted for if it is assumed that the electron is preferentially trapped on a vanadium adjacent to the protonated oxygen and that delocalization is "shut off" between the vanadium atoms bridged by the protonated oxygen.

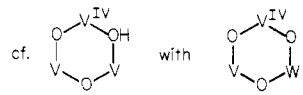

The magnitude of a_{SHF} implies approximately 10% delocalization of electron density on to the vanadium(V) nucleus, and this value is in rough agreement with the valence delocalization parameter α = 0.07 computed from the lowest energy IT band of V_2.[10] At temperatures below 40 K the ESR signals of HV_3 and V_2 are easily

(4) Jortner, J. *J. Chem. Phys.* **1976**, *64*, 4860.
(5) Dawson, B. *Acta Crystallogr.* **1953**, *6*, 113. D'Amour, H. *Acta Crystallogr., Sect. B* **1976**, *B32*, 729.
(6) The synthesis, separation, and characterization of these complexes and their oxidized and reduced isomorphs by elemental analysis, IR, ^{31}P and ^{51}V NMR spectroscopy, cyclic voltammetry, and magnetic susceptibility is described elsewhere (Harmalker, S. P.; Leparulo, M. A.; O'Connor, C. J.; Pope, M. T., manuscript in preparation).
(7) The following parameters were confirmed by simulation of the 5 K spectrum: $g_\parallel$ = 1.927 (2), $g_\perp$ = 1.967 (2), $A_\parallel$ = 160 (1) G, $A_\perp$ = 70 (1) G.
(8) The line width of 30 G required for successful simulation of the spectrum in Figure 2 should be compared with line widths of ca. 10 G observed for the spectra of polyanions containing isolated vanadium(IV) atoms, e.g., α_2-$P_2W_{17}VO_{62}^{8-}$ and α-$PW_{11}VO_{40}^{5-}$.
(9) Parameters for V_2/HV_3 spectra, by simulation: $g_\parallel$ = 1.944 (2), $g_\perp$ = 1.970 (2), $A_\parallel$ = 149 (1) G, $A_\perp$ = 78 (1) G.
(10) $\alpha^2 = (4.24 \times 10^{-4}\, \epsilon_{max} \Delta)/\nu_{IT} d^{2}$.[1,3a] For V_2, ϵ_{max} = 325 M^{-1} cm^{-1}; Δ = 3600 cm^{-1}, ν_{IT} = 8500 cm^{-1}, and d, the V···V separation, is estimated to be 3.4 Å.

saturated, so no spectrum can be observed. At 5 K a rapid passage experiment with low microwave power demonstrates spin flipping for both complexes. To our knowledge this behavior has not been previously observed for mixed-valence species. At 350 K the ESR spectrum of V_2 consists of the expected 15 lines (a = 51 G) for a rapidly hopping electron interacting with two equivalent vanadium nuclei.[11] The corresponding spectrum of HV_3 is much more complex with more than 33 lines. We provisionally ascribe this to the lower symmetry of the protonated V_3O_{13} group which results in unequal interactions of the unpaired electron with the three vanadium nuclei.

Acknowledgment. We thank Dr. Hideo Kon, National Institute for Arthritis and Metabolic Diseases, and Dr. George Yang, Food and Drug Administration, for generously making spectrometers available for some of the ESR measurements and for advice. This research has been supported in part by NSF Grant No. CHE76-19571.

(11) Fifteen- and twenty-two-line spectra per se do not permit us to distinguish unequivocally between rapid electron hopping and electron delocalization (or indeed any combination of these). In the present case we conclude that electron hopping is the predominant mechanism leading to the observed "high-temperature" (300–400 K) spectra because the transition to the "trapped" eight-line spectrum occurs over a temperature range in which the samples are frozen aqueous glycerol glasses (thus ruling out the possibility that slight distortions induced by freezing render the three vanadiums of V_3 inequivalent). We can also show, by observation of unchanged IT spectra of HV_3 in benzene, dimethylformamide, and dimethyl sulfoxide, that the electron "trap" is almost entirely caused by intramolecular polarization and that effects of solvent polarization are negligible.

Bimetallic Catalysts from Pseudotetrahedral Iridium–Tungsten Clusters. Syntheses and Crystal Structures of $(\eta^5\text{-}C_5H_5)WIr_3(CO)_{11}$ and $(\eta^5\text{-}C_5H_5)_2W_2Ir_2(CO)_{10}$

John R. Shapley,* Steven J. Hardwick, Daniel S. Foose, and Galen D. Stucky*‡

Department of Chemistry and Materials Research Laboratory University of Illinois, Urbana, Illinois 61801

Melvyn Rowen Churchill,* Clifford Bueno, and John P. Hutchinson

Department of Chemistry State University of New York at Buffalo Buffalo, New York 14214

Received May 4, 1981

Sinfelt and co-workers[1] have pioneered the development and study of heterogeneous "bimetallic cluster" catalysts, i.e., materials composed of very small bimetallic particles highly dispersed over the surface of an oxide support. These materials customarily have been prepared by simultaneous or sequential impregnation of a separate precursor for each metal, which allows only gross control of stoichiometry. In principle, control of individual particle composition is possible by using appropriate precursor compounds containing both metals, e.g., a bimetallic cluster compound.[2] A critical test of this approach is to compare catalysts derived from two isostructural clusters $[(ML_n)_x(M'L'_m)_y]$, which have a different M/M′ ratio (x/y). Significant effects have been seen for the pair $Co_3Rh(CO)_{12}$ and $Co_2Rh_2(CO)_{12}$ as precursors,[3,4] but

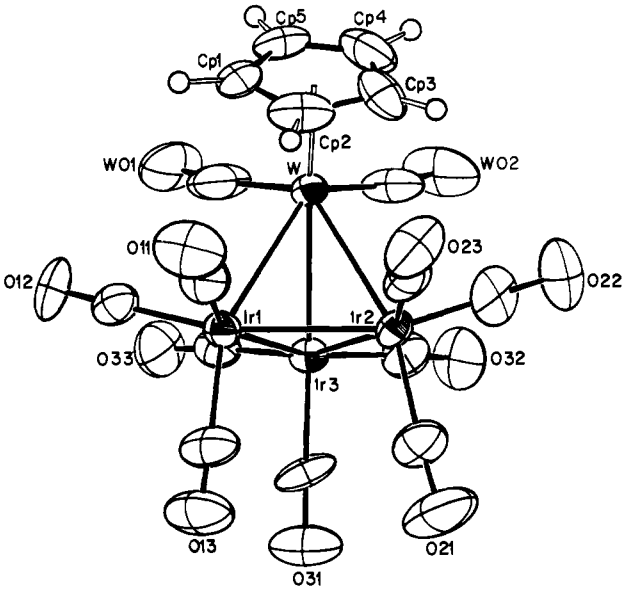

Figure 1. ORTEP diagram of the molecular structure of $CpWIr_3(CO)_{11}$ (**1**). Metal–metal distances within this molecule are Ir(1)–Ir(2) = 2.699 (1), Ir(1)–Ir(3) = 2.702 (1), and Ir(2)–Ir(3) = 2.697 (1) Å [average Ir–Ir = 2.699 (2) Å, compared with 2.693 Å in $Ir_4(CO)_{12}$; W–Ir(1) = 2.815 (1), W–Ir(2) = 2.792 (1), and W–Ir(3) = 2.865 (1) Å (average W–Ir = 2.824 (37) Å].

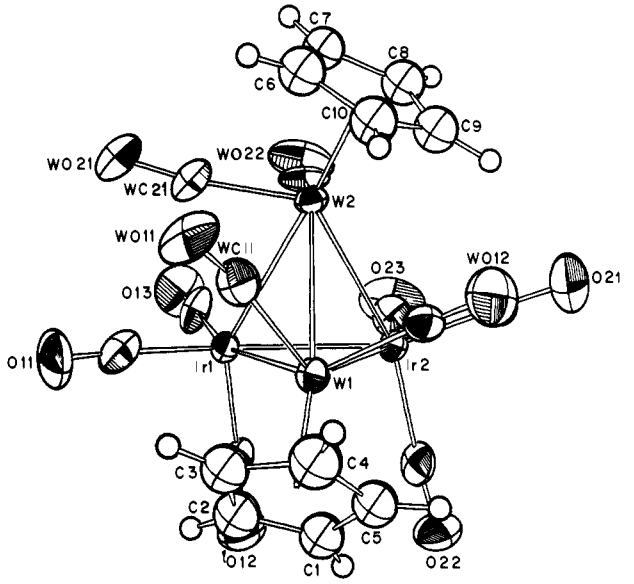

Figure 2. ORTEP diagram of the molecular structure of $Cp_2W_2Ir_2(CO)_{10}$ (**2**). Metal–metal distances within the molecule are W(1)–W(2) = 2.991 (1), Ir(1)–Ir(2) = 2.72 (1), W(1)–Ir(1) = 2.796 (1), W(1)–Ir(2) = 2.833 (1), W(2)–Ir(1) = 2.863 (1), and W(2)–Ir(2) = 2.847 (1) Å (average W(1)–Ir = 2.815, average W(2)–Ir = 2.855 Å).

combinations of less similar transition metals[5] have not been examined. In part this may have been due to the lack of suitable compounds.[6] We now report the convenient syntheses and molecular structures of two tetranuclear iridium–tungsten clusters, $CpWIr_3(CO)_{11}$ (**1**) (Cp ≡ η^5-C_5H_5) and $Cp_2W_2Ir_2(CO)_{10}$ (**2**), together with their use as precursors to alumina-supported bimetallic catalysts.

The combination of $IrCl(CO)_2NH_2C_6H_4Me$ and excess $CpW(CO)_3H$ (CH_2Cl_2, 60 °C, 6 h, 40 psig of CO) in the presence of

‡Central Research and Development Department, Experimental Station, E. I. du Pont de Nemours and Co., Wilmington, DE 19898.

(1) Sinfelt, J. H. *Acc. Chem. Res.* **1977**, *10*, 15 and references therein. Sinfelt, J. H.; Via, G. H. *J. Catal.* **1979**, *56*, 1 and references therein.

(2) Anderson, J. R.; Mainwaring, D. E. *J. Catal.* **1974**, *35*, 162.

(3) (a) Anderson, J. R.; Elmes, P. S.; Howe, R. F.; Mainwaring, D. E. *J. Catal.* **1977**, *50*, 508. (b) Anderson, J. R.; Mainwaring, D. E. *Ind. Eng. Chem. Prod. Res. Dev.* **1978**, *17*, 202.

(4) Ichikawa, M. *J. Catal.* **1979**, *59*, 67.

(5) For the novel use of *potassium* carbonyl ferrates as precursors to Fischer–Tropsch catalysts, see: McVicker, G. B.; Vannice, M. A. *J. Catal.* **1980**, *63*, 25. See also ref 32.

(6) Review of mixed-metal clusters: Gladfelter, W. L.; Geoffroy, G. L. *Adv. Organometal. Chem.* **1980**, *18*, 207.

0002-7863/81/1503-7383$01.25/0